Modification of Pd/CeO$_2$ catalyst by Atomic Layer Deposition of ZrO$_2$

Tzia Ming Onn [a],[*], Lisandra Arroyo-Ramirez [a], Matteo Monai [b], Tae-Sik Oh [a], Meghavi Talati [a], Paolo Fornasiero [b], Raymond J. Gorte [a], Mahmoud M. Khader [c]

[a] Department of Chemical and Biomolecular Engineering, University of Pennsylvania, 34th Street, Philadelphia, PA 19104, USA
[b] Department of Chemical and Pharmaceutical Sciences, ICCOM-CNR, Consortium INSTM, University of Trieste, via L. Giorgieri 1, 34127 Trieste, Italy
[c] Gas Processing Center, College of Engineering, Qatar University, Doha, P.O. Box 2713, Qatar

ARTICLE INFO

ABSTRACT

Modification of a 1 wt% Pd/CeO$_2$ catalyst by Atomic Layer Deposition of thin ZrO$_2$ films was studied. Calcination of the unmodified Pd/CeO$_2$, prepared by precipitation of aqueous Ce(NO$_3$)$_3$ solutions, with Pd added by impregnation, caused a large decrease in surface area and an increase in crystallite size between 673 K and 1073 K; however, catalysts modified by 0.4 nm ZrO$_2$ films showed no change in either surface area or CeO$_2$ crystallite size upon calcination to 1073 K. Methane-oxidation rates in 0.5% CH$_4$ and 5% O$_2$ were slightly lower on the ZrO$_2$-covered catalyst when both materials were calcined at 673 K but the activity of the ZrO$_2$-modified catalyst did not decrease with catalyst calcination temperature. Both catalysts showed good activity for the water–gas-shift reaction but the ZrO$_2$ film improved sulfur tolerance by preventing formation of cerium sulfates.

© 2015 Elsevier B.V. All rights reserved.

1. Introduction

Ceria (CeO$_2$) is well known to be a promoter for a wide range of metal-catalyzed reactions, from the water–gas-shift (WGS) reaction to methane oxidation [1–4]. Indeed, it has been argued that its application as an Oxygen Storage Capacitor (OSC) in three-way automotive catalysts is, at least in part, due to these promotional effects [5,6]. However, there are serious stability issues with ceria. First, under hydrothermal-aging conditions, pure ceria becomes difficult to reduce [7]. Although this has sometimes been reported to be due to loss of surface area, thermodynamic measurements obtained by coulometric titration have shown that well crystallized ceria can only be reduced at much lower P(O$_2$) [8]. In automotive applications, ceria is essentially always used as a solid solution with zirconia, which is known to stabilize the redox properties and surface area of ceria [9]. Second, ceria is highly susceptible to sulfur poisoning. Ceria reacts with SO$_2$ to form sulfates under oxidizing conditions and cerium sulfates transform to an oxysulfide (Ce$_2$O$_2$S) under reducing conditions [10]. The oxysulfide prevents

oxygen-transfer to the metal and effectively poisons reactions that require participation of both the ceria and the metal phases [11].

Stability of oxide phases is also a very large problem in Solid Oxide Fuel Cell (SOFC) cathodes which commonly use nanoscale perovskites to catalyze oxygen reduction and provide electronic conductivity. In the SOFC application, this nanoscale structure must be maintained at high temperatures, typically in the range from 973 to 1073 K. Sintering of the perovskite catalysts under these conditions is a serious problem [12]. However, a recent report showed that the stability of the cathodes could be dramatically enhanced by depositing a 5 nm film of ZrO$_2$ by Atomic Layer Deposition (ALD) [13]. It is not exactly known how the ZrO$_2$ film stabilized the cathode but it seems likely that it helped maintain the surface area and/or the structure of the perovskite. This makes the concept of stabilizing catalysts by ALD intriguing.

ALD is able to form atomic-scale, uniform films by repeated cycles in which the surface is first reacted with an organometallic precursor, which in turn is then oxidized to form the oxide. Reaction of the organometallic precursor with the surface is performed under conditions which limit the reaction to one monolayer, so that the thickness of the final oxide film can be precisely controlled and determined by the number of cycles. Deposition rates typically range from 0.02 to 0.1 nm per cycle, depending on the precursor

[14–17]. ALD has been used in the preparation of catalysts, both to prepare well-dispersed metals [18] and to stabilize metal particles against sintering or leaching [19,20]. A comprehensive review of this topic has recently been published [21].

Modification of ceria catalysts by ALD of zirconia is of interest for multiple reasons. As discussed earlier, zirconia is able to form solid solutions with ceria and stabilize the redox properties of ceria. How ceria would be affected by a film of zirconia is not known but some kind of interaction would be expected. Second, zirconia is a good oxygen-ion conductor but much less reactive than ceria with sulfur-containing molecules. It seems possible that zirconia could allow the transfer of oxygen from the gas phase, to and from ceria, while suppressing formation of cerium sulfates and oxysulfides.

Therefore, the present study was carried out to test the idea that thin zirconia films could enhance the catalytic properties of ceria-supported catalysts. We demonstrate that a 0.4 nm thick, ZrO_2 film improves the structural and thermal stability of a CeO_2 support by suppressing the sintering of the CeO_2 crystallites upon calcination at elevated temperatures. ALD-modified, Pd/CeO_2 catalysts remained catalytically active for methane oxidation and the WGS reaction. Finally, the WGS activity of the ALD-modified catalyst was much more easily regenerated after SO_2 poisoning.

2. Materials and methods

The ceria powder used in this study was prepared by precipitating an aqueous solution of cerium (III) nitrate hexahydrate (10 g, $Ce(NO_3)_3 \cdot 6H_2O$, Sigma Aldrich) with excess ammonium hydroxide (NH_4OH, Fisher Scientific). The resulting precipitate was then dried overnight at 333 K and heated in air at 673 K for 6 h. To test the idea that surface-area stabilization is not simply due to the presence of zirconia, a 50 wt% ceria–zirconia powder, designated here as CZ, was made using similar methods, only mixing zirconyl nitrate hydrate ($ZrO(NO_3)_2 \cdot H_2O$, Sigma Aldrich) with the cerium nitrate in aqueous solution. After calcination to 773 K, XRD patterns of the ceria–zirconia powder showed a single broad peak around 28° 2θ, corresponding to the (1 1 1) reflection, in agreement with formation of a solid solution [22]. 1 wt% Pd was added to each of the resulting powders using incipient wetness of a palladium–citrate salt solution. The Pd salt was decomposed by again calcining the sample to 673 K in air for 6 h.

The equipment and procedures used for ALD of ZrO_2 are described in previous publications [23,24]. The homebuilt ALD system consists of two heated chambers, one for the catalyst sample and one for the organometallic precursor, both of which could be evacuated with a mechanical vacuum pump. High-temperature valves separated the two chambers from each other and from both the vacuum pump and a source of water vapor. After evacuation, the ZrO_2 precursor, (tetrakis(dimethyl amino)-zirconium (TDMZ, Sigma–Aldrich)), was heated to 353 K to produce a TDMZ vapor pressure of approximately 2 Torr. The TDMZ vapor was then admitted into the evacuated sample chamber, which was held at 453 K. The catalyst was exposed to TDMZ vapor for 60 s to ensure that reaction with the solid sample was complete, then evacuated and exposed to water vapor (~100 Torr) for 60 s. After again evacuating the sample, the procedure was repeated. In the present study, 20 cycles were deposited (designated here as $20ZrO_2$-Pd/CeO_2) and the final amount of ZrO_2 on the sample was determined gravimetrically. Multiple samples were prepared as part of this study and the amount of zirconia added corresponded to 11 wt% in each case.

The surface areas of the catalysts were determined from Brunauer–Emmett–Teller (BET) isotherms using N_2 adsorption at 78 K, while powder X-Ray Diffraction (XRD) patterns were recorded from a Rigaku Smartlab diffractometer equipped with a Cu $K\alpha$ source. The Pd dispersions were determined volumetrically using

CO adsorption uptakes at room temperature on the reduced catalyst, using pretreatment procedures discussed elsewhere [25]. X-ray photoelectron spectroscopy (XPS) was carried out in an ultra-high vacuum system with a base pressure of 1×10^{-8} Pa equipped with a dual Mg/Al X-ray source (SPECS XR50), an ion gun (Omicron ISE 10) and an electron/ion energy analyzer (SPECS Phoibos 150). Pd(3d), Ce(3d), Zr(3d), O(1s) and C(1s) levels were probed using an excitation energy of $h\upsilon = 1486.6$ eV (Al $K\alpha$). Binding energies are reported after correction for charging using adventitious C(1s) as a reference.

Steady-state, CH_4 oxidation rates were measured in a 0.25 in., quartz, tubular reactor using helium as the carrier gas with the partial pressures of CH_4 and O_2 fixed at 3.8 Torr (0.5%) and 38 Torr (5%) respectively. The total flow rate of He was kept at 110 mL/min. The steady-state WGS rates were also determined in the same flow reactor with partial pressures of CO and H_2O both at 25 Torr (3.3%). The total flow rate of He, in this case, was kept at 60 mL/min. The mass of catalysts used in every rate measurements were 0.10 g and the products were analyzed using a gas chromatograph (SRI8610C) equipped with a Hayesep Q column and a TCD detector. All rates in this study were normalized to the amount of Pd in the catalyst. Differential conversions were maintained in all cases.

SO_2 poisoning was accomplished by passing 5 mmol of SO_2, generated by reacting sodium bisulfite ($NaHSO_3$, Sigma Aldrich) with sulfuric acid (H_2SO_4, Fisher Scientific), over the 0.1 g sample of catalyst using He in the same flow reactor used for CH_4 oxidation and WGS reactions. The catalysts were then oxidized at various temperatures before again being tested for WGS activity.

Fourier transform infrared spectra (FTIR) were collected on a Mattson Galaxy FTIR with a diffuse-reflectance attachment (Collector II^{TM}) purchased from Spectra-Tech Inc. Spectra were collected at 4 cm^{-1} resolution. The intensities of the spectral features were normalized by making the background peaks between 700 cm^{-1} and 1000 cm^{-1} be identical for all cases.

3. Results

3.1. Characterization of ZrO_2-covered Pd/ceria

Various techniques were used to characterize the Pd/ceria catalyst before and after deposition of 20 ALD cycles (11 wt%) of ZrO_2 ($20ZrO_2$-Pd/CeO_2), and the Pd/ceria–zirconia. First, following calcination at 673 K, SEM measurements on the Pd/ceria and ZrO_2-modified Pd/ceria samples were indistinguishable. The images (Supplemental information, Figs. S1 and S2) showed features that were irregular in shape, with sizes on the order of 10 nm. On the ZrO_2-modified sample, Energy-Dispersive X-Ray Spectroscopy (EDS) showed that Zr was uniformly spread over the entire sample. The presence of ZrO_2 on the ALD-treated sample was further demonstrated by XPS. Fig. 1 shows the Ce 3d and Zr 3d XPS spectra of this sample after calcination to 673 K. The Ce 3d spectra are indicative of a completely oxidized sample, with all of the Ce present in the +4 oxidation state [26]. The Zr 3d doublet shows the typical BE of ZrO_2 and a broadening of the signal probably due to differential charging of the powdered sample [27,28].

BET surface areas were measured on the Pd/ceria, Pd/ceria–zirconia, and ZrO_2-modified Pd/ceria samples as a function of calcination temperature, with results shown in Table 1. The surface area of the fresh Pd/ceria catalyst after calcination at 673 K was 47 m^2/g. Assuming that the surface of the Pd/ceria catalyst is flat compared to the ZrO_2 ALD film and that the ZrO_2 film has the density of tetragonal ZrO_2, the film thickness after 20 cycles can be estimated from the mass increase to be approximately 0.4 nm. This corresponds to a film growth rate of 0.02 nm/cycle, the same value determined in a previous study in which a Pd/Al_2O_3
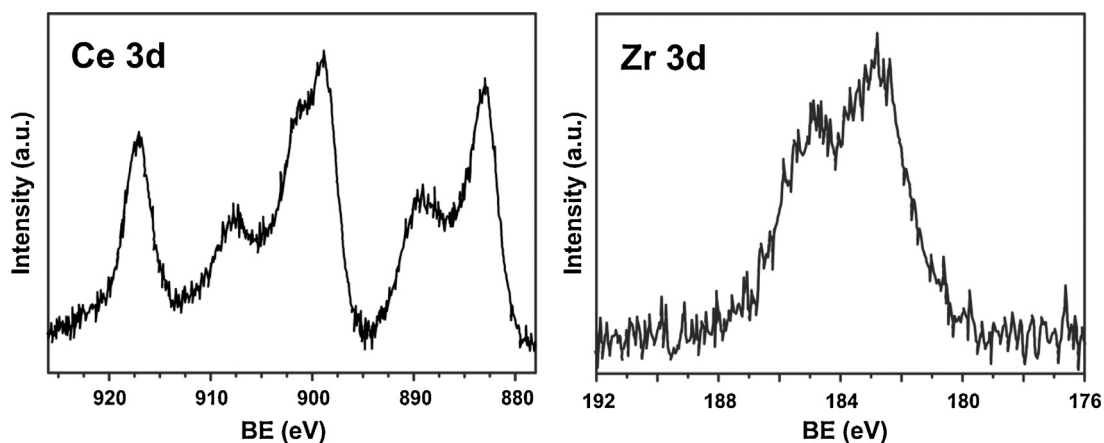
Fig. 1. XPS spectra of Ce 3d and Zr 3d for $20ZrO_2$-Pd/CeO_2 after calcination to 673 K.

Table 1
Surface areas of the samples used in this study after calcination to the indicated temperatures.

Calcination temp. (K)	BET surface area (m^2/g)		
	Pd/CZ	Pd/CeO_2	$20ZrO_2$-Pd/CeO_2
673	70	47	38
773	63	42	41
873	48	36	42
973	40	30	40
1073	30	18	39

catalyst was modified by ZrO_2 ALD [23]. Similar growth rates have also been reported for CeO_2 ALD using similar precursors [24,29,30]. The surface area of ZrO_2-modified catalyst was 38 m^2/g after calcination to 673 K to remove the ligands. Most of the lost specific surface area is accounted for by the increase in sample mass (47 m^2/1.11 g = 42 m^2/g).

The effect of the 0.4-nm ZrO_2 film on the evolution of the Pd/ceria surface area with increasing calcination temperature was surprisingly large. As demonstrated in Table 1, the specific surface area of the unmodified Pd/ceria catalyst declined steadily with increasing calcination temperature, to a value of 18 m^2/g after heating to 1073 K in air. On a percentage basis, the loss in surface area of the Pd/ceria–zirconia sample was similar, decreasing from 70 m^2/g to 30 m^2/g after calcination at 1073 K, demonstrating that the solid solution is not qualitatively different from ceria with regards to its sintering resistance. However, the ZrO_2-covered Pd/ceria showed no change in surface area with increasing calcination temperature, remaining 39 m^2/g after heating to 1073 K.

A further indication of the stabilizing effect of the 0.4 nm ZrO_2 film is shown by the XRD data in Fig. 2. The XRD patterns of the unmodified and ZrO_2-covered Pd/ceria after calcination at 673 K were indistinguishable. The patterns showed only broad peaks associated with the fluorite structure of ceria and no evidence for either Pd or ZrO_2. For this Pd loading, no peaks associated with Pd are expected. The absence of ZrO_2 peaks implies that the ZrO_2 remains amorphous or is present as a thin film. Fig. 2 is a plot of the width at half maximum for the (1 1 1) peak at 28° 2θ, along with the corresponding crystallite size calculated from that peak width using the Scherrer Equation, for both samples as a function of calcination temperature. Not surprisingly, the XRD patterns of the unmodified Pd/ceria sharpened with increasing calcination temperature, implying that sintering caused an increase in the crystallite size from an initial value of 18 nm to 32 nm after calcination at 1073 K. This is in agreement with the loss in surface area this sample experienced. However, within experimental uncertainty,
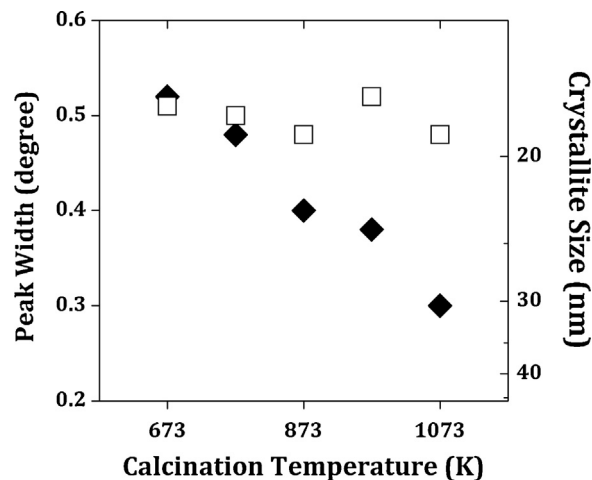

Fig. 2. Peak width at half maximum height and crystallite size obtained from XRD patterns of (□)—$20ZrO_2$-Pd/CeO_2 and (♦)—Pd/CeO_2 sample at 2θ = 28.54° as a function of calcination temperature.

Table 2
Pd dispersions as a function of sample calcination temperature.

Calcination temp. (K)	Metal dispersion (%)	
	Pd/CeO_2	$20ZrO_2$-Pd/CeO_2
673	50	23
773	40	28
873	35	30
1073	30	28

the XRD patterns of the ZrO_2-modified Pd/ceria were unaffected by increasing calcination temperature.

Since the ZrO_2 coatings will also affect the Pd, dispersion measurements were performed on the Pd/ceria and ALD-modified Pd/ceria catalysts as a function of calcination temperature using CO chemisorption at room temperature, with results shown in Table 2. In a procedure described elsewhere [25], the catalysts were first reduced in H_2 at 673 K before cooling to room temperature and measuring CO uptakes. The reduction step is necessary to reduce PdO to Pd and therefore to prevent reaction of CO to CO_2, which could then adsorb on the reduced ceria surface. The Pd dispersion was initially 50% on the unmodified catalyst but this reduced steadily to 30% after calcination 1073 K. On the ZrO_2-modified catalyst, the initial dispersion was only 23% but this increased to 28% after calcination to 773 K and remained constant at this value. We suggest that the dispersions were lower on the modified catalyst
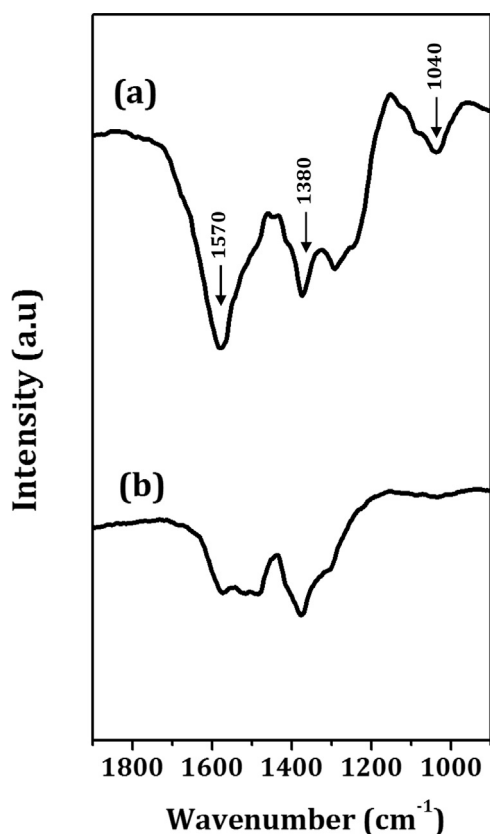
Fig. 3. DRIFTS spectra obtained for (a) Pd/CeO_2 and (b) $20ZrO_2$-Pd/CeO_2, after exposure to 10% CO in flowing He at 573 K for 10 min.

Table 3
Steady-state, water–gas-shift activity for the unmodified and ZrO_2-modified Pd/ceria and after SO_2 poisoning and oxidative regeneration.

Water gas shift activity at 573 K (10^{16} CO molecules/s/g.cat)			
	Fresh activity	After SO_2 poisoning	Regeneration
$20ZrO_2$-Pd/CeO_2	99	17	80
Pd/CeO_2	100	1.3	2.8

because the Pd was partially covered by ZrO_2. The small increase with increasing calcination temperature was likely due to partial removal of the ZrO_2 film. In the previous study in which Pd/Al_2O_3 was modified by ALD of ZrO_2 [23], the dispersion was lower than that of the unmodified catalyst and also increased with calcination temperature. In that case, the increase in dispersion was larger, probably because the sample had been treated with 50 ALD cycles.

To determine how the presence of the ZrO_2 film might affect the surface properties of the Pd/ceria catalyst, we performed FTIR measurements following catalyst reductions in CO. The Pd/ceria and ZrO_2-modified Pd/ceria catalysts were first calcined in air at 673 K to ensure that they were completely oxidized, then placed in the FTIR cell and reduced in 10% CO–He mixtures. Spectra were collected after flushing in dry He. For unmodified Pd/ceria, reduction of PdO and CeO_2 in CO produces CO_2, which in turn reacts with the reduced ceria to form carbonates [31]. This is shown in spectrum of Fig. 3(a), which exhibits broad features between $1300 cm^{-1}$ and $1700 cm^{-1}$. In the analogous spectrum of the ZrO_2-modified catalyst, Fig. 3(b), these peaks are significantly reduced in intensity. Since we will later show that the ZrO_2-modified catalyst is catalytically active, we suggest that the ZrO_2 film prevents formation of cerium carbonates by covering a significant fraction of the ceria surface.

3.2. Catalytic properties

The effect of modifying the catalyst by ALD of ZrO_2 was examined using methane oxidation with 0.5% CH_4 and 5% O_2. Differential rates for the unmodified and ZrO_2-modified catalysts are shown in Fig. 4 following catalyst calcination to either 673, 973, or 1073 K. Considering the results on unmodified Pd/ceria, Fig. 4(a), there is a progressive decline in activity with calcination temperature, as

indicated by the need to go to increasingly higher temperatures to achieve the same rates. The sample calcined at 1073 K required temperatures that were approximately 100 K higher in order to achieve a particular rate compared to the catalyst calcined at 673 K. At a given temperature, the rate decreased by more than an order of magnitude. Since the decrease in rates was much greater than the decrease in ceria surface area or the decrease in Pd dispersion, other factors must also be involved. Interestingly, the activation energy remained 90 ± 10 kJ/mol and did not change with calcination temperature. Methane-oxidation rates have been reported to depend on Pd crystallite size [32], support reducibility [33,34], and support-metal interfacial contact area [35]. Apparently, increasing the calcination temperature changed more than just the surface area and dispersion and these changes dramatically reduced the methane oxidation activity.

The activity of the ZrO_2-modified catalyst is somewhat lower than that of the fresh Pd/ceria, as shown in Fig. 4(b). For catalysts calcined at 673 K, the rates on the ZrO_2-modified catalyst were a factor of about two lower than that of the unmodified catalyst; the activation energy, 65 kJ/mol, was also lower. However, the rates on the modified catalyst did not change significantly with calcination temperature. Because of this, the ZrO_2-modified sample exhibited rates that were almost an order of magnitude higher after the two catalysts were calcined at 1073 K, even though the Pd dispersion on the modified catalyst was lower. Again, other factors must be important for determining the activity of these materials.

The earlier observation that carbonate formation is suppressed on the ZrO_2-modified catalyst led us to consider whether the ZrO_2 layer might also reduce the effects of sulfur poisoning. Sulfur poisoning has previously been shown to have a very large effect on the WGS activity of Pd/ceria [11] and it has been suggested that this decrease in activity is related to the loss in OSC in working catalysts. Therefore, we measured WGS rates on unmodified and ZrO_2-modified Pd/ceria, before and after exposure to SO_2. Rates were measured at 573 K in 25 torr each of H_2O and CO and the catalysts were poisoned by simply exposing them to a 5 mmol "slug" of SO_2 at 573 K. Because Pd can also be poisoned by sulfur but regenerated by oxidation treatments, the poisoned catalysts were oxidized in flowing, 5% O_2 at 973 K for 30 min. The WGS rates on the two catalysts after these pretreatments are reported in Table 3. Prior to SO_2 exposures, the two catalysts exhibited nearly identical WGS rates. After SO_2 exposure, both catalysts lost most of their activity. However, the ZrO_2-modified sample was nearly completely restored after oxidation at 973 K, while the unmodified Pd/ceria remained inactive.

To better understand the differences, we performed FTIR measurements on the two catalysts after the above pretreatments, with results shown in Fig. 5. After SO_2 poisoning at 573 K, the FTIR spectrum of the unmodified Pd/ceria catalyst showed intense bands at $1160 cm^{-1}$ and $1250 cm^{-1}$. These can be identified as being due to sulfates on the ceria. Heating in 5% O_2 at 973 K for 30 min did not significantly change the spectrum. The ZrO_2-modified catalyst also showed strong bands due to sulfate formation after SO_2 exposure; however, the intensity of these bands decreased dramatically upon oxidation at 973 K. While it was not possible for us to quantify the SO_2 coverages based on the FTIR results, it appears that sulfates
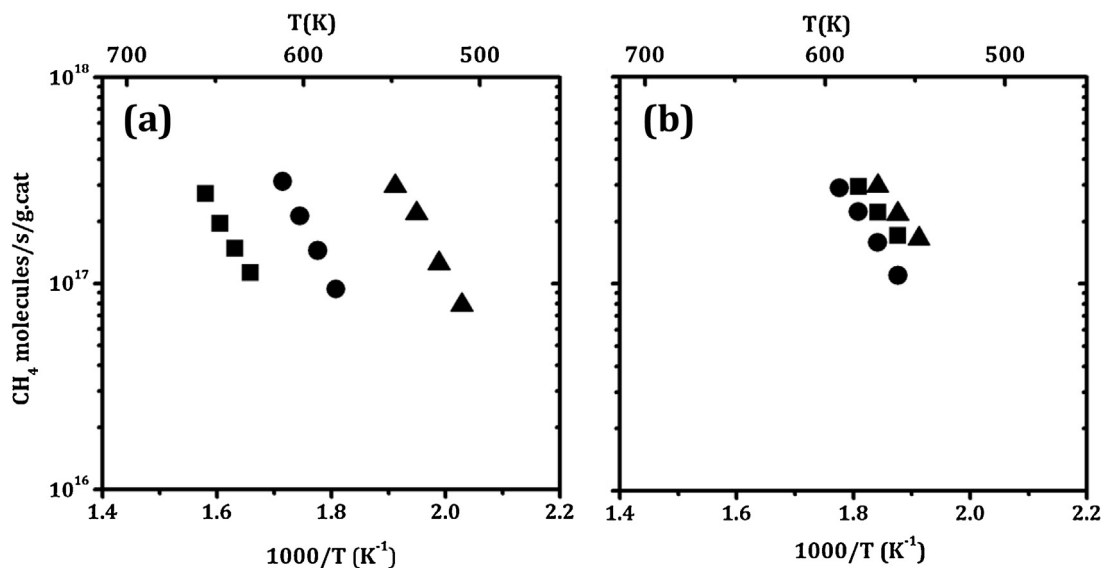
Fig. 4. Steady-state, differential methane oxidation rates in 0.5% CH_4 and 5% O_2. (a) CH_4 oxidation rates on Pd/CeO_2 after calcination to the following temperatures: (▲)—673 K, (●)—973 K, and (■)—1073 K. (b) Rates on $20ZrO_2$-Pd/CeO_2 after calcination to the following temperatures: (▲)—673 K, (●)—973 K, and (■)—1073 K.
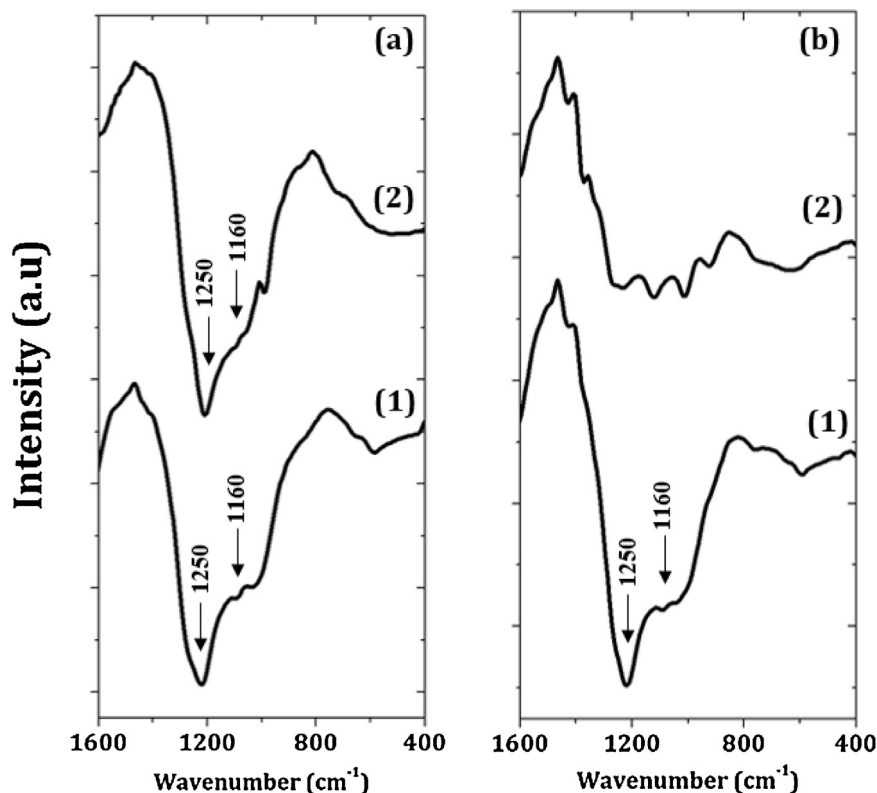

Fig. 5. DRIFTS spectra of (a) Pd/CeO_2 and (b) $20ZrO_2$-Pd/CeO_2 after (1) exposure to a slug of SO_2 at 573 K for 30 min and (2) heating in 5% O_2 at 973 K for 30 min.

can be formed on the ZrO_2 but that these decompose much more readily.

4. Discussion

Atomic Layer Deposition is receiving an increasing amount of attention as a way of preparing and modifying catalysts [21]. The self-limiting reactions of precursors with surfaces allow catalytic materials to be prepared with a control over structure and composition that is not possible with most other synthesis methods. The present work demonstrates several advantages that can be gained by catalyst modification using ALD.

First, by depositing an oxide that is a catalyst promoter, it is possible to increase the activity of supported-metal catalysts. Previous publications have already shown that intimate contact between Pd and ZrO_2 can promote methane-oxidation activity [35] and that ALD of ZrO_2 is a convenient way of preparing materials in which ZrO_2 and Pd are in close contact [23]. The present work extends that idea in that the deposited oxide can also interact with the oxide phase, CeO_2 in this case. Ceria–zirconia mixed oxides are well

known to exhibit enhanced reducibility [9]. Therefore, some of the enhanced rates in the present study may result from the contact between CeO_2 and ZrO_2.

Second, the fact that a ZrO_2 film, only one unit cell in thickness, can so dramatically stabilize the surface area and crystallite size of polycrystalline CeO_2 was a surprise. Previous reports that SOFC cathode performance could be stabilized by ZrO_2 overlayers used much thicker films, on the order of 5 nm, and only inferred stabilization of the surface area based electrode performance [13]. It seems unlikely that the ZrO_2 film has significant mechanical strength, so that the mechanism by which ZrO_2 stabilizes CeO_2 is likely associated with changing the surface energy of the system. Sintering results from a material minimizing its free energy by decreasing the surface energy. However, if the surface energy is already low, the driving force for sintering will decrease. We suggest a mechanism of this type must be involved in the surface stabilization of CeO_2 by ZrO_2. The ZrO_2 must be decreasing the surface energy of the ceria.

Third, the present study demonstrated that thin oxide films deposited by ALD can provide a very effective chemical barrier to prevent poisoning of a catalyst, without significantly affecting catalytic activity for the desired reaction. Here, we demonstrated that the ZrO_2 film improved the sulfur tolerance of CeO_2 but the concept may apply in other cases as well. The ability of ALD to form a uniform, continuous film over the entire catalyst surface makes it uniquely capable of preparing materials with these properties.

The present study demonstrates the exciting possibilities that are offered by using ALD to modify catalysts. Clearly, the field is still in its infancy, with many more advantages waiting to be found.

5. Conclusions

Modification of a Pd/CeO_2 catalyst by thin, ALD-deposited ZrO_2 films leads to several improvements in the catalyst performance. First, the films stabilize the surface area and crystallite size of the ceria. Second, they enhance the catalytic activity for the methane-oxidation reaction on catalysts that have been calcined to higher temperatures. Third, the ZrO_2 films improve the sulfur tolerance of the catalysts by preventing formation of cerium sulfates. The work further demonstrates that ALD is an important tool for catalyst synthesis.

Acknowledgements

Appendix A. Supplementary data

Supplementary data associated with this article can be found, in the online version, at http://dx.doi.org/10.1016/j.apcatb.2015.12.028.

References

[1] R.J. Gorte, AIChE J. 56 (2010) 1126–1135.
[2] A. Trovarelli, Catal. Rev. 38 (1996) 439–520.
[3] C.M. Kalamaras, S. Americanou, A.M. Efstathiou, J. Catal. 279 (2011) 287–300.
[4] K.C. Petallidou, A.M. Efstathiou, Appl. Catal. B: Environ. 140 (2013) 333–347.
[5] T. Bunluesin, R. Gorte, G. Graham, Appl. Catal. B: Environ. 14 (1997) 105–115.
[6] T. Bunluesin, R. Gorte, G. Graham, Appl. Catal. B: Environ. 15 (1998) 107–114.
[7] J. Kašpar, P. Fornasiero, M. Graziani, Catal. Today 50 (1999) 285–298.
[8] G. Zhou, P.R. Shah, T. Montini, P. Fornasiero, R.J. Gorte, Surf. Sci. 601 (2007) 2512–2519.
[9] P. Fornasiero, G. Balducci, R. Di Monte, J. Kašpar, V. Sergo, G. Gubitosa, A. Ferrero, M. Graziani, J. Catal. 164 (1996) 173–183.
[10] T. Luo, J.M. Vohs, R.J. Gorte, J. Catal. 210 (2002) 397–404.
[11] T. Luo, R.J. Gorte, Catal. Lett. 85 (2003) 139–146.
[12] W. Wang, M.D. Gross, J.M. Vohs, R.J. Gorte, J. Electrochem. Soc. 154 (2007) B439–B445.
[13] Y. Gong, D. Palacio, X. Song, R.L. Patel, X. Liang, X. Zhao, J.B. Goodenough, K. Huang, Nano Lett. 13 (2013) 4340–4345.
[14] M. Coll, J. Gazquez, A. Palau, M. Varela, X. Obradors, T. Puig, Chem. Mater. 24 (2012) 3732–3737.
[15] A. Marizy, T. Désaunay, D. Chery, P. Roussel, A. Ringuedé, M. Cassir, ECS Trans. 57 (2013) 983–990.
[16] A. Marizy, P. Roussel, A. Ringuedé, M. Cassir, J. Mater. Chem. A 3 (2015) 10498–10503.
[17] Z. Fan, C.-C. Chao, F. Hossein-Babaei, F.B. Prinz, J. Mater. Chem. 21 (2011) 10903–10906.
[18] S.T. Christensen, J.W. Elam, F.A. Rabuffetti, Q. Ma, S.J. Weigand, B. Lee, S. Seifert, P.C. Stair, K.R. Poeppelmeier, M.C. Hersam, Small 5 (2009) 750–757.
[19] T.D. Gould, A. Izar, A.W. Weimer, J.L. Falconer, J.W. Medlin, ACS Catal. 4 (2014) 2714–2717.
[20] B.J. O'Neill, D.H. Jackson, A.J. Crisci, C.A. Farberow, F. Shi, A.C. Alba-Rubio, J. Lu, P.J. Dietrich, X. Gu, C.L. Marshall, Angew. Chem. 125 (2013) 14053–14057.
[21] B.J. O'Neill, D.H. Jackson, J. Lee, C. Canlas, P.C. Stair, C.L. Marshall, J.W. Elam, T.F. Kuech, J.A. Dumesic, G.W. Huber, ACS Catal. 5 (2015) 1804–1825.
[22] V.S. Escribano, E.F. López, M. Panizza, C. Resini, J.M.G. Amores, G. Busca, Solid State Sci. 5 (2003) 1369–1376.
[23] T.M. Onn, S. Zhang, L. Arroyo-Ramirez, Y.-C. Chung, G.W. Graham, X. Pan, R.J. Gorte, ACS Catal. 5 (2015) 5696–5701.
[24] S.Y. Anthony, R. Küngas, J.M. Vohs, R.J. Gorte, J. Electrochem. Soc. 160 (2013) F1225–F1231.
[25] X. Wang, R.J. Gorte, J. Wagner, J. Catal. 212 (2002) 225–230.
[26] T. Skála, F. Šutara, K.C. Prince, V. Matolín, J. Electron Spectrosc. Relat. Phenom. 169 (2009) 20–25.
[27] Y. Mi, J. Wang, Z. Yang, Z. Wang, H. Wang, S. Yang, RSC Adv. 4 (2014) 6060–6067.
[28] K. Kuratani, M. Uemura, M. Mizuhata, A. Kajinami, S. Deki, J. Am. Ceram. Soc. 88 (2005) 2923–2927.
[29] M. Coll, J. Gazquez, A. Palau, M. Varela, X. Obradors, T. Puig, Chem. Mater. 24 (2012) 3732–3737.
[30] A. Marizy, P. Roussel, A. Ringuedé, M. Cassir, J. Mater. Chem. A 3 (2015) 10498–10503.
[31] S. Hilaire, X. Wang, T. Luo, R. Gorte, J. Wagner, Appl. Catal. A: Gen. 215 (2001) 271–278.
[32] P. Briot, M. Primet, Appl. Catal. 68 (1991) 301–314.
[33] W.R. Schwartz, D. Ciuparu, L.D. Pfefferle, J. Phys. Chem. C 116 (2012) 8587–8593.
[34] D. Ciuparu, E. Perkins, L. Pfefferle, Appl. Catal. A: Gen. 263 (2004) 145–153.
[35] C. Chen, Y.-H. Yeh, M. Cargnello, C.B. Murray, P. Fornasiero, R.J. Gorte, ACS Catal. 4 (2014) 3902–3909.